

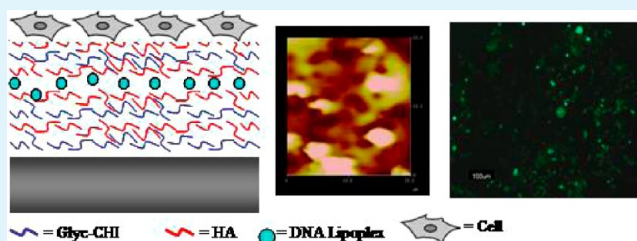
Substrate-Mediated Gene Delivery from Glycol-Chitosan/Hyaluronic Acid Polyelectrolyte Multilayer Films

Christina A. Holmes[†] and Maryam Tabrizian^{*,†,‡}

[†]Department of Biomedical Engineering and [‡]Faculty of Dentistry, Duff Medical Science Building, 3775 University Street, McGill University, Montreal, H3A 2B4, Canada

ABSTRACT: Substrate-mediated transfection is one of the key strategies for localized gene delivery. Layer-by-layer (LbL) polyelectrolyte deposition is a promising technique which enables controlled delivery of a number of biofactors, including nucleic acids. Here, we embed lipoplexes containing plasmid DNA within polyelectrolyte multilayers composed of glycol-chitosan (Glyc-CHI) and hyaluronic acid (HA) in order to produce a film system that enables localized, surface-based transfection. The topography and morphology of the resulting multilayers were characterized after lipoplex absorption and during subsequent film build-up via atomic force microscopy (AFM) and scanning electron microscopy (SEM), respectively. DNA embedding efficiency and release were then examined. Lipoplex-containing Glyc-CHI/HA films were found to successfully transfect NIH3T3 fibroblasts and HEK293 kidney cells in vitro, maintaining transfection levels of approximately 20% for a period of at least 7 days.

KEYWORDS: gene delivery, lipoplex, substrate-mediated, layer-by-layer deposition, glycol-chitosan



INTRODUCTION

Spatial control of gene delivery is an essential feature of many biomedical applications, including inductive tissue engineering, medical implant coatings, and cellular transfection microarrays. One main approach to localized gene transfer, termed “substrate-mediated gene delivery”¹ or “reverse-transfection”,² involves the immobilization of DNA and carrier vectors onto a biomaterial surface, as opposed to the traditional “bolus” transfection method of adding the DNA and vector to an aqueous media. A variety of strategies can be employed to surface-immobilize gene transfection vectors, including non-specific absorption,³ surface attachment via biotin-streptavidin¹ and antibody–antigen conjugate systems,⁴ or encapsulation within a thin polymeric or hydrogel film.² Among these many methods, layer-by-layer polyelectrolyte deposition has emerged as a simple yet versatile technique which can be utilized with biomaterials of nearly any type, shape, or size.

Layer-by-layer (LbL) deposition involves the sequential surface assembly of alternating layers of oppositely charged polyelectrolytes (PEs)⁵ and has been widely used for the controlled release of drugs, bioactive proteins, and genes (reviewed in ref 6). Naked plasmid DNA, PEI- and cyclodextran-complexed plasmids, and adenoviral vectors have been incorporated into a variety of polyelectrolyte multilayer designs (reviewed in ref 7) and have been successfully used to transfect cells in vitro and in vivo.^{8,9} Careful selection of the PEs used and the layer architecture and chemistry employed enables both the tailoring of release kinetics and sequential delivery of several different genes.^{10,11}

Plasmid DNA itself is often directly used as the anionic PE for LbL assembly, alongside degradable cationic polymers. For

example, Lynn and colleagues built PE multilayers from a synthetic hydrolytically degradable cationic polyamine (“polymer 1”) and naked plasmid DNA encoding EGFP or RFP,¹² which, used alone or as a stent-coating, could transfect cells in vitro¹³ and in vivo.⁹ Atomic force microscopy (AFM) analysis suggested that the DNA/polymer layers rearranged themselves to present surface-bound condensed DNA nanoparticles.¹³ Naked plasmid DNA-based LbL multilayers have also been constructed using chitosan,¹⁴ galactosylated chitosan,¹⁵ poly(2-aminoethyl propylene phosphate),¹⁶ poly(ethylimine),¹⁷ and reducible hyperbranched poly(amido amine)⁸ as the cationic PEs, with similar film surface rearrangements into nanoparticle complexes observed in most cases. As these plasmid-cationic polymer films degrade, these complexes are released, as verified via electrophoresis and transmission electron microscopy (TEM)^{15,16} and are thought to act like other typical cationic gene delivery vectors.

Alternatively, plasmids precomplexed with a viral or nonviral gene carrier vector can also be incorporated within multilayer films for controlled, substrate-mediated transfection. The Voegel and Jessel groups, for example, have done extensive work using PLL/PGA, chitosan (CHI)/hyaluronic acid (HA), PAH/PSS, and PLL/HA multilayer films to deliver PEI-condensed plasmids,¹⁸ pyridylamino cyclodextrin complexed plasmids,¹¹ or adenoviral vectors¹⁹ to several different cell lines as well as primary cells. While results varied greatly between systems, generally, lower transfection levels were observed

Received: May 30, 2012

Accepted: January 2, 2013

Published: January 2, 2013

when the vector was embedded under greater numbers of PE bilayers, and an increase in the number of vector layers led to an increase in transfection efficiency.^{11,18,19}

Few studies to date have attempted to incorporate DNA-lipoplexes within LbL PE films, even though lipid-based DNA carriers are the most widely used nonviral vectors. Several other strategies have been used to immobilize DNA-lipoplexes to biomaterial surfaces, with most studies focusing on surface adsorption^{3,20,21} or physical incorporation within cast films.^{22,23} As a coating enabling stent-based gene delivery, Yaumuchi and co-workers have used LbL deposition to assemble alternating layers of DNA-containing lipoplexes and naked plasmid DNA on top of self-assembled monolayers of carboxylic acid-terminated alkanethiol. The resulting multilayers were able to successfully transfect HEK293 and HUVEC cells in vitro with EGFP at high efficiencies, with continued EGFP expression for a period of over 9 days in the case of films composed of 5 layers.²⁴ While this film system shows promise, it uses a high concentration of DNA in production and is limited in the types of release profiles it can yield. It would thus be of great interest to incorporate DNA-containing lipoplexes within a biocompatible PE film, rather than composing the multilayer itself entirely of DNA and lipoplexes.

As gene delivery vectors do not diffuse readily through most LbL multilayer systems, it is crucial to select PEs that allow for controlled film dissolution under physiological conditions. The biodegradable, naturally derived polysaccharides chitosan (CHI) and hyaluronic acid (HA) have been incorporated into multilayer film architectures for a variety of bioapplications, including successful in vitro transfection when incorporating adenoviral or PEI-condensed vectors.^{11,18} However, studies have indicated that many cell lines exhibit decreased adhesion to CHI/HA multilayer films, particularly as the number of layers are increased,²⁵ thus suggesting transfection from these films may be far from optimal. We have recently developed an alternative film system utilizing glycol-modified chitosan (Glyc-CHI) and have demonstrated that Glyc-CHI/HA films exhibit significantly improved cellular adhesion compared to corresponding films consisting of unmodified chitosan, while maintaining many of their physical properties.²⁶ Here we incorporate lipoplexes consisting of plasmid DNA complexed with the widely studied lipid-based gene carrier Lipofectamine 2000 within Glyc-CHI/HA multilayers. The topography, morphology, and DNA release profiles of the resulting LbL films are then characterized, and the multilayer system is then used to successfully transfect NIH3T3 fibroblasts and HEK293 kidney cells in vitro.

MATERIALS AND METHODS

Materials. Hyaluronic acid (HA) with a molecular weight of 74 kDa was purchased from Lifecore Biomedical (Chaska, MN, USA). Glycol-Chitosan (Glyc-CHI) with a molecular weight of approximately 80 kDa (via gel permeation chromatography (GPC)) was purchased from Sigma-Aldrich. The plasmid encoding enhanced green fluorescent protein (pEGFP-C3) was acquired from Clontech (CA, USA). Lipofectamine 2000 and subcloning efficiency DH5 α competent *E. coli* cells were obtained from Invitrogen (CA, USA). NIH3T3 mouse embryonic fibroblast cells and HEK293 human embryonic kidney cells were supplied by American Type Culture Collection (ATCC, VA, USA). Sodium dodecyl sulfate (SDS) and sodium chloride (NaCl) were purchased from Sigma-Aldrich; cell culture cover glasses (15 mm, round) were obtained from Fisher Scientific.

Plasmid Amplification and Purification. The 4.7 kb plasmid encoding enhanced green fluorescent protein (pEGFP-C3), driven by a human cytomegalovirus promoter (CMV) and containing a kanamycin resistance gene, was amplified in DH5 α cells in the presence of kanamycin. Plasmid purification was performed using a Plasmid Maxi Prep Kit (Quiagen, CA, USA) according to manufacturer instructions, and the resulting plasmid DNA (pDNA) was resuspended in MillQ water. The pDNA concentration and purity was measured using a UV spectrophotometer at 260 and 280 nm.

Formation and Characterization of DNA Lipoplexes. All lipoplexes were prepared at room temperature in a 0.1 M NaCl buffer solution, adjusted to pH 6.0 and filtered through a 0.22 μ m PES stericup filtration unit (Milipore), at a ratio of 2 μ L of Lipofectamine 2000 to 1 μ g of pEGFP. Briefly, two solutions of equal volume (150 μ L in the case of film formation and 500 μ L in the case of particle characterization) were prepared, one containing either 1, 2, 4, or 6 μ g of pEGFP DNA and the other containing 2, 4, 8, or 12 μ L of Lipofectamine 2000 (i.e., at a ratio of 2 μ L of lipid to 1 μ g of plasmid, as recommended by the product datasheet), and left to stand for 10 min. These two solutions were then combined and incubated at room temperature for 15 min, before immediate use in the formation of films or for lipoplex characterization.

The average hydrodynamic diameter and polydispersity of the DNA lipoplexes were determined via low angle dynamic light scattering (DLS) at room temperature at a 90° angle (90Plus, Brookhaven Instruments, NY, USA), while the lipoplex surface charge was characterized via zeta potential measurement (ZetaPALS, Brookhaven Instruments, NY, USA). DLS and zeta measurements were performed in a 0.1 M NaCl buffer solution, pH \sim 6.0.

LbL Assembly of Films. Both Glyc-CHI and HA polyelectrolyte solutions were prepared at a concentration of 2 mg/mL in 0.1 M NaCl buffer, adjusted to pH 6.0 and filtered through a 0.22 μ m PES stericup filtration unit (Milipore). Prior to film deposition, cover glasses were cleaned in 10 mM SDS for three hours, rinsed in distilled water three times, treated with 0.1 N HCl overnight and thoroughly rinsed in distilled water. LbL build up was achieved using the pipet approach, wherein 300 μ L of each polymer solution was deposited directly onto the cover glass, beginning with the polycation (Glyc-CHI). After the polymer was allowed to adsorb for 10 min, the polymeric films were rinsed twice in 0.1 M NaCl buffer. Then, the polyanion, HA, was added, allowed to adsorb for 10 min and rinsed twice. This was repeated at each step of LbL deposition until five bilayers of film, with an additional terminating layer of Glyc-CHI, i.e. [Glyc-CHI/HA]₅Glyc-CHI, was formed. The selection of approximately five underlying bilayers was made since Glyc-CHI/HA films of this thickness (\sim 100 nm) had been previously characterized²⁶ as providing good substrate coverage. Next, 300 μ L of DNA-Lipoplex solution, containing 2, 4, or 6 μ g of pEGFP, was added to the films, allowed to adsorb for 2 h, and rinsed once in 0.1 M NaCl buffer. These DNA lipoplex containing films were then either used as is, or covered with a further 2 or 4 bilayers and a terminating layer of Glyc-CHI, thus forming: [Glyc-CHI/HA]₅Glyc-CHI-Lipo or "surface adsorbed" films; [Glyc-CHI/HA]₅Glyc-CHI-Lipo-[Glyc-CHI/HA]₂Glyc-CHI or "two overlying bilayer" films; and [Glyc-CHI/HA]₅Glyc-CHI-Lipo-[Glyc-CHI/HA]₄Glyc-CHI films or "four overlying bilayer" films, respectively.

Atomic Force Microscopy. The topography of DNA lipoplex containing Glyc-CHI/HA films was imaged by atomic force microscopy (AFM) in "wet" conditions using the Nanoscope III (Digital Instruments, USA) system in tapping mode. Samples were analyzed within a multimode fluid cell (model MTFML, Veeco) filled with 0.1 M NaCl solution (pH 6), using a silicon nitride probe with a nominal spring constant of 0.3 N/m and a nominal radius of curvature of 20 μ m (model NP, Veeco). A 20 μ m \times 20 μ m area was scanned at a rate of 1 Hz using the minimum amount of force required to obtain steady images. Mean RMS surface roughness was calculated using Nanoscope v 5.12r5 software.

Scanning Electron Microscopy. DNA lipoplex-containing film morphology was characterized with a Hitachi S-4700 field emission gun scanning electron microscope (FEG-SEM). Prior to imaging, film

samples were dehydrated in an increasing series of ethanol solutions (30–100% in water); with a 10 min incubation for each step in the series. Samples were then critically point dried in CO₂ and gold–palladium-coated, via sputter coating under an argon atmosphere, prior to SEM analyses.

Quantification of DNA Film Content and Release. DNA lipoplex containing Glyc-CHI/HA films were formed on cover glasses placed within 24 well tissue culture plates (Falcon) and incubated in 1 × PBS solution, pH = 7.4, at 37 °C in a humidified atmosphere of 5% CO₂. The supernatant was removed and replaced with fresh PBS solution each day. The amount of DNA within the supernatant was measured via the Quant-iT PicoGreen assay (Molecular Probes, Invitrogen) according to manufacturer specifications. Briefly, an equal volume of 0.2% w/v heparin sulfate (Sigma) solution in 2 × TE buffer was added to the supernatant solution (final concentration of 0.1% w/v heparin in 1 × TE buffer) in order to decomplex the plasmid from the lipoplex, thus allowing the PicoGreen stain access to the DNA. Fluorescence was then measured using a fluorescent plate reader (Flx800, Bio-Tek Instruments, VT, USA) using excitation and emission wavelengths of ~480 and ~520 nm, respectively. A series of DNA standards in 0.1% w/v heparin, 1 × TE buffer was produced and measured for reference.

In order to indirectly measure the quantity of DNA embedded within the Glyc-CHI/HA films, the plasmid content of the lipoplex solution before and after deposition, as well as the DNA concentration of the rinsate was measured via the PicoGreen assay as described above.

Cell Culture and Transfection. NIH3T3 mouse embryonic fibroblast cells and HEK293 human embryonic kidney cells (ATCC) were grown in Dulbecco's minimum essential medium (DMEM, ATCC) supplemented with 10% fetal calf serum (FCS, ATCC) and 1% penicillin/streptomycin (Invitrogen) and incubated at 37 °C in a humidified atmosphere of 5% CO₂.

[Glyc-CHI/HA]₅Glyc-CHI-Lipo, [Glyc-CHI/HA]₅Glyc-CHI-Lipo-[Glyc-CHI/HA]₂Glyc-CHI, and [Glyc-CHI/HA]₅Glyc-CHI-Lipo-[Glyc-CHI/HA]₄Glyc-CHI films, containing 2, 4, or 6 μg of pEGFP, were built in 24 well tissue culture plates (Falcon), as described above with a few modifications. After the first three bilayers of film were formed (i.e., [Glyc-CHI/HA]₃), samples were sterilized with 70% (v/v) ethanol for 30 min and then washed in the following ethanol series for 15 min each: 50%, 20%, and 10%. To ensure complete removal of the ethanol, substrates were then washed three times (5 min each wash) in 0.1 M NaCl buffer, pH 6. Film deposition then continued under sterile conditions and using sterile solutions, with a polyelectrolyte deposition time of 20 min employed for the first sterile bilayer (i.e., the fourth bilayer) and 10 min used for all subsequent bilayers. It should be noted that during the washing and media equilibration steps, all of the substrates, including the controls, were treated in the same manner.

After film formation, NIH3T3 or HEK293 cells were prepared for seeding. Cells were trypsinized and spun down at 1000 rpm for 5 min, resuspended in fresh media, and the cell concentration was determined using a hemocytometer. A seeding population of 5 × 10⁴ cells (in a volume of 500 μL) was added to each of the wells and incubated at 37 °C in a humidified atmosphere of 5% CO₂ for 2, 4, or 7 days, with media exchange being performed every 2 days. As a positive control, bolus transfections were performed on cells seeded on [Glyc-CHI/HA]₅Glyc films. Briefly, 25 μL solutions containing 2 μg of pEGFP and 4 μL of Lipofectamine 2000 were prepared separately in 0.1 M NaCl buffer (pH = 6.0), combined and incubated at room temperature for 15 min, and added to the seeded cells. Additional controls included cells seeded on [Glyc-CHI/HA]₅Glyc films, those seeded on [Glyc-CHI/HA]₅Glyc-CHI-Lipo*-[Glyc-CHI/HA]₂Glyc-CHI films, where the lipoplexes were formed with blank plasmid DNA in place of pEGFP, and cells seeded on [Glyc-CHI/HA]₅Glyc-CHI-DNA*-[Glyc-CHI/HA]₂Glyc-CHI films, where 4 μg of pEGFP plasmid DNA was adsorbed in the absence of any lipid carrier.

Fluorescence Microscopy. Fluorescent images of transfected cells after 2, 4, or 7 days were acquired with a stereoscopic zoom microscope (SMZ1500, Nikon) equipped with a high pressure mercury lamp (C-SHG1, Nikon; USA), the appropriate set of filters

for fluorescein (FITC) excitation and emission, and a digital camera (DXM1200F, Nikon) operated with ACT-1 software.

Fluorescent Activated Cell Sorting Analysis. Cellular transfection efficiency and cytotoxicity after 2, 4, or 7 days was assessed via fluorescent activated cell sorting (FACS). After removing the media, samples were rinsed once in PBS and cells were trypsinized for 5 min (0.05% trypsin-EDTA, Invitrogen). Next, 1 mL of 2% FBS in PBS was added to each well and cells were spun down at 250g for 5 min. Cells were then resuspended in 300 μL of 2% FBS in PBS, transferred into FACS tubes, and 3 μL of 40 μg/mL propidium iodide (PI) was added to each sample. Samples were then directly FACS analyzed using the BD FACS Calibur system (BD Biosciences, USA), equipped with a 488 nm argon laser to excite both PI and GFP, with 10 000 cells per sample assessed. FACS data was subsequently analyzed for GFP and PI expression using FlowJo software (Treestar Inc., OR, USA), using appropriate gates and controls.

Statistics. Statistical analyses of data were performed using the software package SPSS/PASW Statistics v18.0 (SPSS Inc., Chicago, IL). All data are presented as mean ± standard deviation (STD). The significance level was set at *p* < 0.05. As most data either failed the Shapiro–Wilk test for normality and/or Levene's test for homogeneity of variance, or were of small sample size, Kruskal–Wallis non-parametric analyses were performed.

■ RESULT AND DISCUSSION

Lipoplex and Film Characterization. The size, surface charge, and polydispersity of the lipoplexes used in this study, formed from the complexation of plasmid DNA encoding enhanced green fluorescent protein (pEGFP) with Lipofectamine 2000, are presented in Table 1. Increasing the amount of

Table 1. Physical Characterization of pEGFP Containing Lipoplexes^a

amount of DNA (μg)	avg particle diameter (nm)	avg zeta potential (mV)	avg polydispersity index
2	360 ± 59	-44 ± 4	0.25 ± 0.01
4	585 ± 54	-46 ± 1	0.31 ± 0.01
6	754 ± 59	-38 ± 3	0.30 ± 0.01

^aLipoplexes were formed at a ratio of 2 μL of Lipofectamine 2000 to 1 μg of plasmid using the indicated amount of DNA. The size and polydispersity of the resulting complexes were determined via low angle dynamic light scattering (DLS), while particle surface charge was characterized via zeta potential measurement. Data presented is from three separate experiments (n = 9).

DNA increased the resulting lipoplex size, from 360 ± 59 nm in diameter for 2 μg of plasmid to 754 ± 59 nm for 6 μg, while the polydispersity index remained fairly constant. All lipoplexes exhibited a net negative surface charge, around -40 mV, and were thus subsequently sandwiched between polycationic Glyc-CHI layers when forming LbL films.

Previous studies of DNA–Lipofectamine 2000 complexes have yielded both negatively charged^{3,23,27} and positively charged²⁸ particles, broadly ranging in hydrodynamic diameter from 100 to 1000 nm.^{23,27–29} The observed wide variety in lipoplex properties, including those seen in this study, are mainly due to differences in the conditions employed for particle formation, including: the size, type, and amount of plasmid used; the ratio of lipid to DNA utilized; the volume and properties of the solution in which they are complexed (e.g., presence of serum and/or ionic species such as calcium, pH); and complexation time.

Atomic force microscopy (AFM) images of surface adsorbed (Figure 1B–D), two bilayer overlying (E–G), and four bilayer

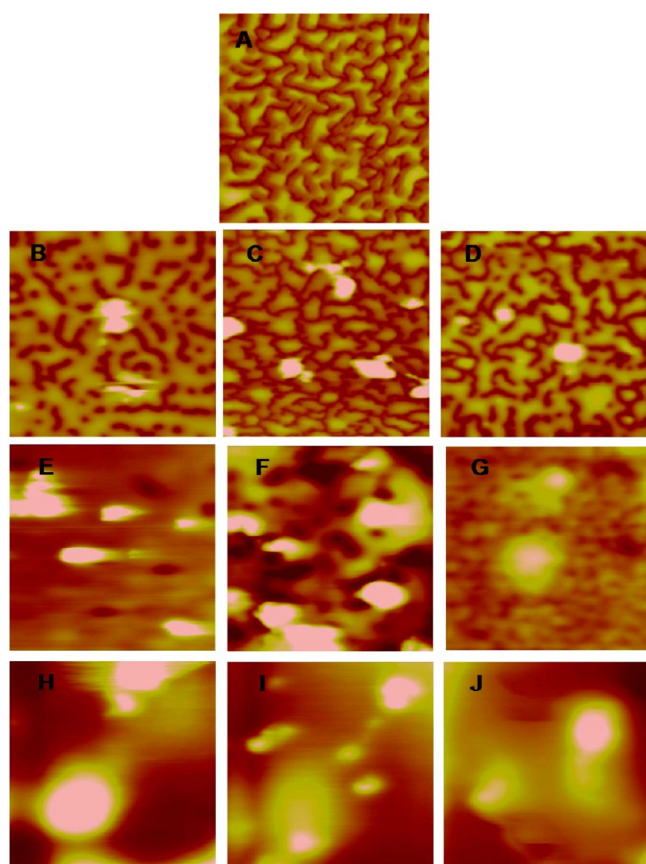


Figure 1. AFM imaging of the surface topography of polyelectrolyte films constructed using 2 (B, E, H), 4 (C, F, I), or 6 μg (D, G, J) of pEGFP DNA. Lipoplexes formed using the indicated amounts of DNA were adsorbed on the surface of $[\text{Glyc-CHI/HA}]_5\text{Glyc-CHI}$ films (B, C, D) and, then, covered with a further two (E, F, G) or 4 film bilayers (H, I, J). A close-up scan of a $[\text{Glyc-CHI/HA}]_5\text{Glyc-CHI}$ film without any adsorbed lipoplexes is presented for comparison (A). Scan size = 20 μm (B–J), Z range = 250 (A, C), 350 (B, D–F, H, I), or 450 nm.

overlying (H–J) films revealed that DNA lipoplexes tended to adsorb upon the multilayer surface (A) as large (averaging 2–3

μm) aggregates of varying size, as opposed to individual particles with sizes similar to the effective hydrodynamic diameters determined via DLS analysis. In the case of the surface adsorbed films, the AFM images also clearly displayed the structure of the underlying film, visible underneath, and surrounding the large adsorbed particles, which was similar to that of bare $[\text{Glyc-CHI/HA}]_5\text{Glyc-CHI}$ films (Figure 1A) and to that observed in our previous studies.²⁶ As the DNA–lipoplexes were covered with an increasing number of bilayers (center and bottom), the areas surrounding the particles gradually appear smoother.

This coating over of the surface-bound lipoplexes is more apparent on scanning electron microscopy (SEM) images (Figure 2). SEM of PE multilayers formed with 4 μg of DNA revealed that DNA–Lipofectamine 2000 complexes adsorbed on the film surface as clusters of smaller particles of varying size, often joined together via strandlike structures (Figure 2A and D). These details of particle structure become less distinct as the lipoplexes are covered with a further two (Figure 2B and E) and then four (Figure 2C and F) bilayers of PE film. The clustered globule-like appearance of the surface adsorbed DNA–Lipofectamine 2000 complexes observed here is very similar to that seen via SEM for comparable particles composed of DNA and various lipids.^{30,31}

The presence of large lipoplex aggregates forming on the PE film surface is not entirely surprising due to the long particle adsorption time used. DNA–lipid complexes are often known to form aggregates with time after preparation, particularly at high concentrations, which is one of the reasons they are prepared fresh before use.³² Indeed, our lipoplexes formed using 4 μg of DNA were found to aggregate in solution from an average diameter of 585 ± 54 nm, to approximately 1081 ± 18 nm after 1 h and to around 1291 ± 48 nm after 2 h. Interactions between the lipid portion of the DNA complexes and the underlying PE layer may also contribute to aggregation or lipoplex deformation at the film surface. Previous studies of unilamellar lipid vesicles embedded within PGA/PAH films similarly showed vesicle fusion or aggregation into structures much larger (400–1000 nm) than those of individual vesicles in solution (200 nm).³³

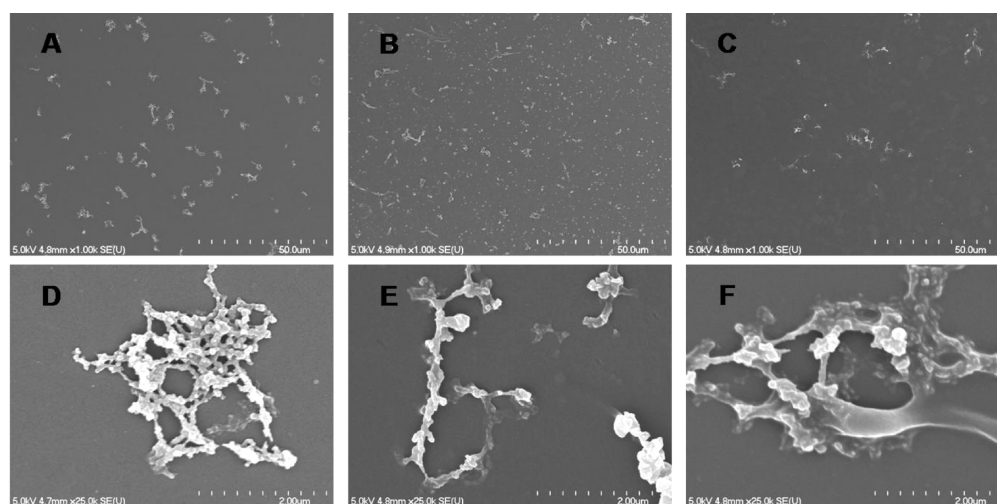


Figure 2. SEM images of film morphology of polyelectrolyte films constructed using 4 μg of pEGFP at 1000 times (A–C) and 25 000 times (D–F) magnification. Lipoplexes were adsorbed on the surface of $[\text{Glyc-CHI/HA}]_5\text{Glyc-CHI}$ films (A and D), and then covered with a further two film bilayers (B and E) or four film bilayers (C and F).

Lipoplex Embedding Efficiency and DNA Release. By measuring the DNA concentration, via the PicoGreen assay, of the lipoplex solution before and after deposition, as well as the DNA concentration of the rinsate, the actual pEGFP content within the PE films was indirectly determined. Films formed with 2 μg of plasmid were found to contain 712 ± 44 ng of DNA, representing an embedding efficiency of 32%, while those built with 4 and 6 μg contained 1259 ± 175 ng (31%) and 1271 ± 417 ng (21%), respectively. The electrostatically mediated adsorption of lipoplexes thus appears to saturate at approximately 600 ng/cm^2 of DNA for this Glyc-CHI/HA film system. In comparison, previous work examining surface absorption of DNA–Lipofectamine 2000 complexes to tissue culture plastic found that 2 h of incubation yielded a DNA surface density of around $200\text{--}300 \text{ ng/cm}^2$, which rose significantly to approximately $4 \mu\text{g/cm}^2$ after 24 h of absorption.³ As in our study, the adsorbed DNA density was found to depend upon the quantity of DNA used; however, in direct contrast to our results, lower amounts of incubated plasmid (0.5 vs 2 μg) resulted in greater overall DNA density and loading efficiency.³ Yamauchi and co-workers, meanwhile, achieved a DNA surface density of under 300 ng/cm^2 for the LbL deposition of 3 layers of lipoplexes, which were alternated with 2 layers of free plasmid, in their stent coating study.²⁴

DNA release from “2 μg ”, “4 μg ”, and “6 μg ” [Glyc-CHI/HA]₅Glyc-CHI-Lipo, [Glyc-CHI/HA]₅Glyc-CHI-Lipo-[Glyc-CHI/HA]₂Glyc-CHI, and [Glyc-CHI/HA]₅Glyc-CHI-Lipo-[Glyc-CHI/HA]₄Glyc-CHI films incubated in PBS, pH = 7.4, at 37 °C was measured each day for a period of 1 week (Figure 3). All films were found to be fairly stable, with less than 5% of

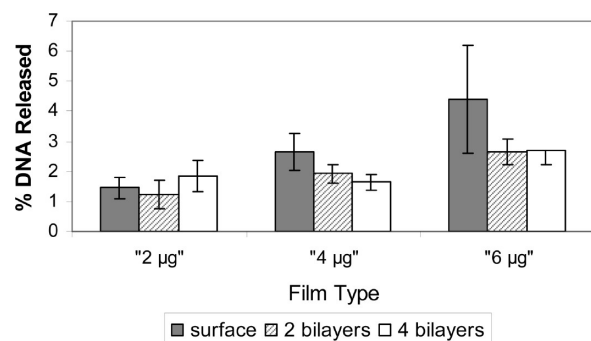


Figure 3. Cumulative DNA released over 7 days for Glyc-CHI/HA films constructed using 2, 4, or 6 μg of pEGFP and with the following architectures: [Glyc-CHI/HA]₅Glyc-CHI-Lipo (filled) or [Glyc-CHI/HA]₅Glyc-CHI-Lipo[Glyc-CHI/HA]_NGlyc-CHI films, where $N = 2$ (lines) or 4 (empty). DNA released into the PBS supernatant was measured via the PicoGreen assay each day, and the cumulative amount released over 7 days was calculated and compared to the amount of DNA embedded within each film. Data presented represents the mean \pm STD for three separate experiments ($n = 9$).

embedded DNA released cumulatively by day 7 for any film type. Unsurprisingly, in the case of maximally loaded “4 μg ” and “6 μg ” films, less DNA was released when the lipoplexes were embedded within two or four bilayers than when the lipoplexes were simply adsorbed onto the surface, although increasing the number of overlying layers appeared to have little effect. Meanwhile, in the nonsaturated “2 μg ” films, the presence of overlying film layers did not seem to have a direct effect on DNA release. These results bear resemblance to previous studies, where $\sim 6\%$ of DNA from the lipoplexes adsorbed to

tissue culture plastic were released in PBS over 1 week,³ and less than 10% of adsorbed DNA was released in PBS for a single layer of lipoplexes in the stent coating study.²⁴

Transfection Efficiency and Cytotoxicity. Initial 48 h transfection studies performed using NIH3T3 fibroblast cells revealed a significant difference in transfection efficiency as the amount of DNA used to construct the film varied ($\chi^2 = 26.277$, $p < 0.001$). More specifically, an increase in transfection efficiency was observed between 2 and 4 μg films, but no significant increase was observed for 6 μg films, with a maximum transfection efficiency of approximately 14% (Figure 4A). These results closely reflect the observed saturation in

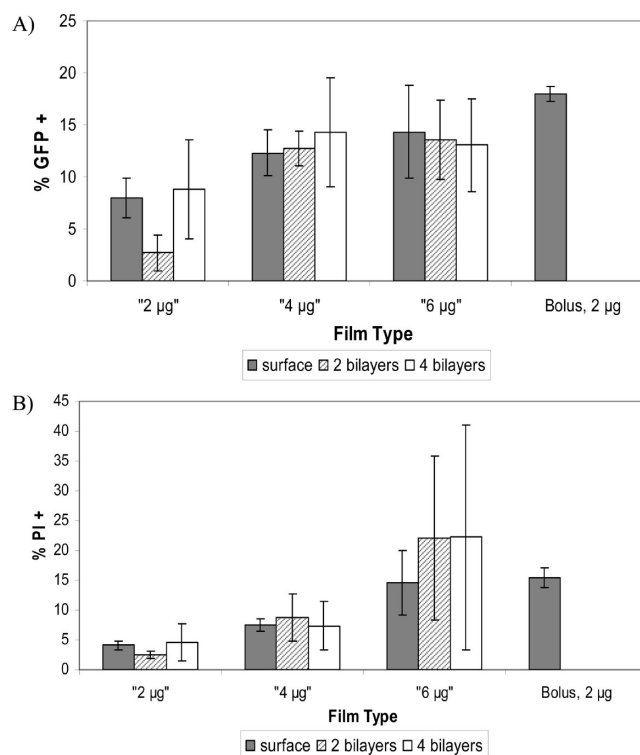


Figure 4. NIH3T3 transfection efficiency (A) and death (B) after 48 h of growth on [Glyc-CHI/HA]₅Glyc-CHI-Lipo[Glyc-CHI/HA]_NGlyc-CHI films, where $N = 0$ (filled), 2 (lines), or 4 (empty). Lipoplexes were formed from the indicated amount of pEGFP. Data presented represent the mean percentage of GFP-expressing (A) or PI-staining (B) cells, as determined via fluorescent activated cell sorting, \pm STD for three separate experiments ($n = 9$). (Stats, for amount of DNA $\chi^2 = 26.277$, $p < 0.001$ for GFP, $\chi^2 = 40.130$, $p < 0.001$ for PI; for no. of bilayers $\chi^2 = 1.552$, $p = 0.460$ for GFP; $\chi^2 = 0.35$, $p = 0.983$ for PI.)

DNA content between 4 and 6 μg films, as mentioned above. Films constructed using lipoplexes containing blank plasmid DNA yielded no detectable GFP expression, while those consisting of 4 μg of uncomplexed plasmid DNA exhibited less than 1% transfection efficiency (data not shown). This latter result clearly indicates that, as is the case with bolus transfection, the presence of a lipid carrier is required in this multilayer film system in order to maximize substrate-based transfection efficiency.

Film cytotoxicity was also found to increase along with the amount of DNA used to construct the films ($\chi^2 = 40.130$, $p < 0.001$), with a maximum of 22% of cells staining for PI (Figure 4B). This continued increase in cytotoxicity even after DNA saturation is achieved may be due to a possible increase in lipid

content between 4 and 6 μg films. Interestingly, overall there was no significant difference between films where the lipoplexes were simply surface adsorbed or films with two or four overlying bilayers ($\chi^2 = 1.552$, $p = 0.460$ for GFP; $\chi^2 = 0.35$, $p = 0.983$ for PI). However, when solely examining films constructed using 2 μg of pEGFP, a decrease in transfection efficiency when surface adsorbed lipoplexes were covered with two bilayers was observed, which recovered to initial levels when covered with four bilayers. Positive controls, consisting of NIH3T3 cells seeded on [Glyc-CHI/HA]₅Glyc-CHI films and bolus transfected with lipoplexes prepared with 2 μg of DNA, yielded a transfection efficiency of approximately 18% and 23% PI staining. It is important to note that our bolus transfection conditions involved cell-lipoplex contact in serum-containing media for the entire 48 h experimental period. This likely accounts for the lower transfection efficiency and higher cytotoxicity observed here in comparison to typical bolus transfection studies which involve 4–8 h of contact in serum-free media.

Higher transfection efficiencies were observed for HEK293 cells 48 h post-transfection (Figure 5). Again the amount of DNA employed in constructing the film had a significant effect ($\chi^2 = 32.890$, $p < 0.001$), with an increase in transfection efficiency observed between 2 and 4 μg films, and no significant

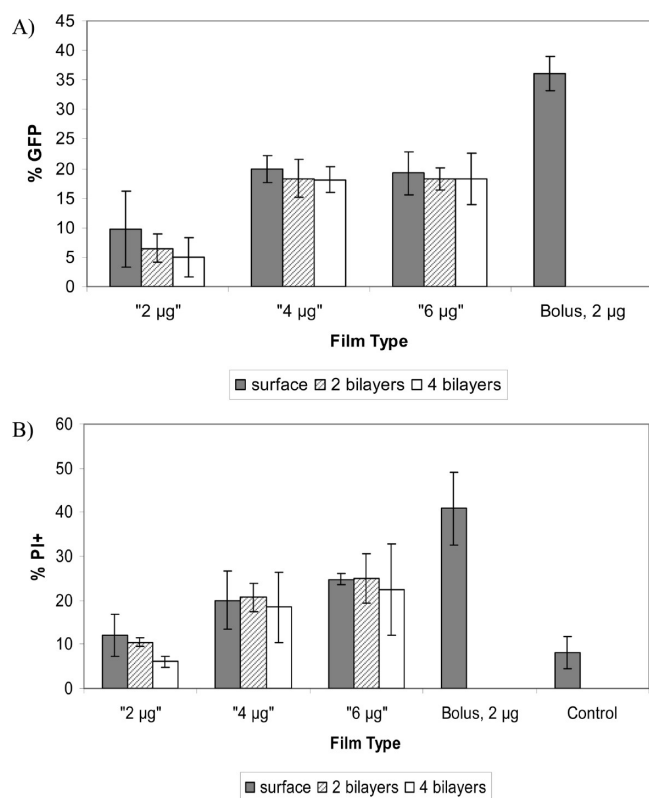


Figure 5. HEK293 transfection efficiency (A) and death (B) after 48 h of growth on [Glyc-CHI/HA]₅Glyc-CHI-Lipo[Glyc-CHI/HA]_NGlyc-CHI films, where $N = 0$ (filled), 2 (lines), or 4 (empty). Lipoplexes were formed from the indicated amount of pEGFP. Data presented represent the mean percentage of GFP-expressing (A) or PI-staining (B) cells, as determined via fluorescent activated cell sorting, \pm STD for two separate experiments ($n = 6$). (HEK293 stats, for amount of DNA $\chi^2 = 32.890$, $p < 0.001$ for GFP, $\chi^2 = 28.104$, $p < 0.001$ for PI; for no. of bilayers $\chi^2 = 2.402$, $p = 0.301$ for GFP; $\chi^2 = 1.373$, $p = 0.503$ for PI.)

increase for 6 μg films. However, this time a maximum transfection efficiency of over 20% was observed. A similar increase in film cytotoxicity alongside increasing amount of incubated DNA was also exhibited (Figure 5B), with a maximum of 25% of cells staining for PI ($\chi^2 = 28.104$, $p < 0.001$). Also similar to results for NIH3T3 fibroblasts, no significant differences between films with zero, 2, or 4 overlying bilayers were generally observed ($\chi^2 = 2.402$, $p = 0.301$ for GFP; $\chi^2 = 1.373$, $p = 0.503$ for PI), with the exception of films constructed with 2 μg of DNA. However, in this case, the transfection efficiency and cytotoxicity decreased with the addition of overlying bilayers. Bolus transfected HEK293 cell controls yielded a transfection efficiency of approximately 36% alongside 41% PI staining. Again the lower bolus transfection efficiency and higher cytotoxicity observed compared to typical bolus experiments is likely due to the extended period of cell contact.

Given that the transfection efficiencies exhibited by HEK293 cells were higher than those observed for NIH3T3 cells, all transfection studies of further time points were conducted solely with HEK293 cells. Also, since no significant increase in transfection efficiency was observed between 4 and 6 μg films, we present time course transfection data for 4 μg films only.

Examining film-based transfection 2, 4, and 7 days post-transfection via fluorescence microscopy suggests an increase in the number of GFP expressing cells with time (Figure 6A). When the actual transfection efficiency is measured via FACS analysis (Figure 6B, left), this increase in transfection efficiency is found to be significant ($\chi^2 = 6.908$, $p = 0.032$), although smaller ($\sim 4\%$ maximum difference between day 2 and 7) than apparent from microscopy. Likewise, cytotoxicity, as indicated by the number of PI staining cells (Figure 6B, right), was found to be maximal (up to $\sim 8\%$ difference between days 2 and 7) for all film types on day 7 ($\chi^2 = 17.397$, $p < 0.001$). This increase in cytotoxicity over time may be due to the prolonged contact time between the lipoplexes and the cells.

While covering the lipoplexes with layers of PE film might intuitively be expected to somewhat delay transfection, this effect was not observed. Instead, although there was little difference on day 2 post-transfection, by days 4 and 7 the transfection efficiency was found to be lower as the number of overlying film bilayers increased, with the greatest difference observed on day 7 ($\chi^2 = 9.191$, $p = 0.01$). These observed reductions in transfection efficiency were small (maximum $\sim 6\%$ between no covering layers and four covering bilayers), yet unexpected. Meanwhile, overall the number of overlying bilayers was found to have no statistically significant effect on cytotoxicity ($\chi^2 = 4.260$, $p = 0.119$), even though on day 7 films with four covering bilayers appear to show $\sim 7\%$ less PI than films with no covering bilayers.

The small but significant decrease in transfection efficiency observed with increasing bilayer coverage for days 4 and 7 post-transfection could be due to a combination of factors. For example, any destabilizing interactions between the lipoplexes and PE layers are likely to be greater as the number of overlying bilayers is increased, and this effect may further be exacerbated with time. It is also possible that lower amounts of plasmid DNA were actually embedded in films with higher numbers of covering bilayers, since the increased number of washing steps during preparation could have leached out DNA. The lack of anticipated time delay in transfection with increasing film coverage, on the other hand, may be due to an insufficient number of overlying bilayers or the time period we chose to

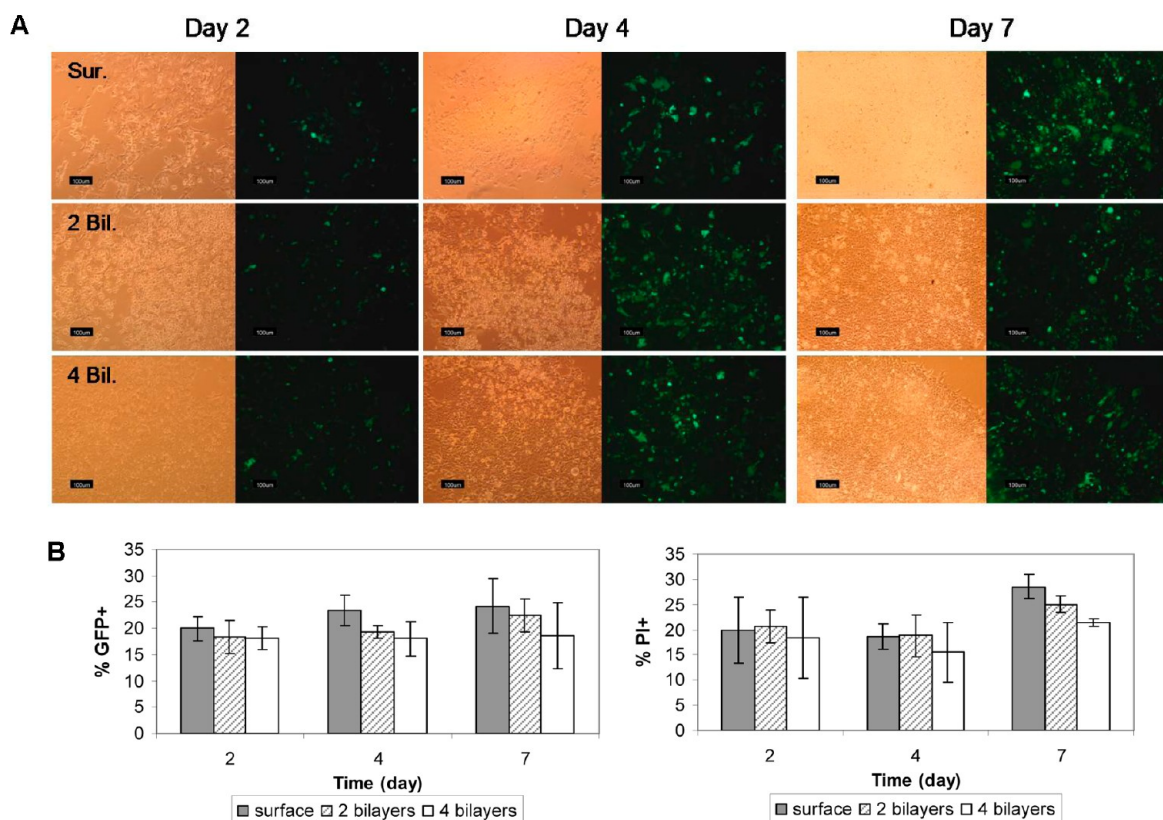


Figure 6. (A) Representative bright field and fluorescence microscopy images of HEK293 cells after 2 (left), 4 (center), and 7 (right) days on polyelectrolyte films constructed using 4 μ g of pEGFP, and with the following architectures: [Glyc-CHI/HA]₅Glyc-CHI-Lipo (top) or [Glyc-CHI/HA]₅Glyc-CHI-Lipo[Glyc-CHI/HA]_NGlyc-CHI films, where $N = 2$ (center) or 4 (bottom). (B) HEK293 transfection efficiency (left) and death (right) over time on [Glyc-CHI/HA]₅Glyc-CHI-Lipo[Glyc-CHI/HA]_NGlyc-CHI films, where $N = 0$ (filled), 2 (lines), or 4 (empty). Lipoplexes were formed from 4 μ g of pEGFP. Data presented represent the mean percentage of GFP-expressing (top) or PI-staining (bottom) cells, as determined via fluorescent activated cell sorting, \pm STD ($n = 6$). (Stats for no. of bilayers $\chi^2 = 9.191$, $p = 0.01$ for GFP, $\chi^2 = 4.260$, $p = 0.119$ for PI; for day $\chi^2 = 6.908$, $p = 0.032$ for GFP, $\chi^2 = 17.397$, $p < 0.001$ for PI.)

observe. For comparison, sequential transfection of COS cells was achieved over a time scale of 2–8 h in an influential study which embedded two cyclodextrin complexed plasmids, one encoding EGFP and the other a nuclearly expressed protein, within PLGA/PLL films.¹¹ The film architecture employed in that case sandwiched each plasmid layer between five bilayers of film, similar to our four overlying bilayer films, thus suggesting that in our study we may have looked too late to detect any differences in transfection kinetics between our films with surface adsorbed vs embedded lipoplexes.

As has been found in other studies,³⁴ the transfection observed from our lipoplex containing films appears to be mediated via direct cellular contact and/or interaction with the film rather than lipoplex diffusion. This is suggested by the observed stability of our films in PBS over a period of over 1 week, as well as preliminary studies conducted in serum-free media. In these experiments, lipoplex containing Glyc-CHI/HA films were incubated in serum-free media for 2 days. When the collected supernatant from this period of incubation was added to control HEK293 cells grown on tissue culture plastic, no transfection was observed (data not shown). However, when HEK293 cells were seeded on the remaining films, successful substrate-mediated transfection was achieved, albeit at lower efficiencies than those observed on fresh films (data not shown).

The transfection efficiencies achieved by our lipoplex film system may at first glance appear lower than those obtained by

both the previously mentioned tissue culture plastic-adsorbed lipoplex study³ and the LbL-based lipoplex stent coating study,²⁴ which yielded transfection efficiencies of $\sim 30\%$ in NIH3T3 cells and $\sim 80\%$ in HEK293 cells, respectively. However, it is difficult to directly compare these results with ours due to the differing analysis methods used. In the former study, for example, the plasmid that was delivered encoded for luciferase and thus transfection was assessed via a luminometer.³ In the latter case, although an analogous gene encoding GFP was used, transfection efficiency was measured via randomized manual count of fluorescent microscopy images,²⁴ which may somewhat overestimate the number of GFP positive cells and does not take into account autofluorescence. However, in our work FACS analysis, a far more accurate technique for quantifying both transfection efficiency and cell death within the same samples, was employed. Additionally, the maximal $\sim 80\%$ transfection observed in the LbL stent coating study was for five layer films which contain three layers of lipoplexes and two layers of plasmid DNA.²⁴ When only a single layer of lipoplexes was used, a transfection efficiency similar to that observed here, $\sim 20\%$, was found. This suggests that increasing the number of lipoplex-containing layers in our LbL film system might also significantly increase the transfection efficiency that can be achieved. Finally, while transfection for the LbL stent coating system peaked at day 3 post-transfection and gradually decreased with time,²⁴ our system was able to maintain

transfection levels (or even increase them slightly) over at least 7 days.

CONCLUSIONS

In this study we have successfully incorporated lipoplexes containing plasmid DNA within Glyc-CHI/HA polyelectrolyte multilayer films. We have further demonstrated that this lipoplex film system can be used to transfect both NIH3T3 fibroblasts and HEK293 kidney cells in vitro, with the transfection efficiency varying depending on the cell type. Films supported transfection for a period of at least 7 days, with a small but statistically significant increase in efficiency and cytotoxicity observed over time. While the number of overlying film bilayers had no significant effect on transfection efficiency or cytotoxicity at 2 days post-transfection, by day 7 there was a small but significant decrease in transfection observed as the adsorbed lipoplexes were covered by greater number of bilayers. Future work with this film system will focus on incorporating more plasmid layers and varying the films architecture in order to achieve sequential gene delivery of multiple genes and a wider variety of transfection kinetic profiles. The lipoplex-containing Glyc-CHI/HA film system could easily be adapted to serve as a coating for stents, orthopedic implants, or 3D tissue engineering scaffolds, thus making it an attractive candidate for use in a variety of gene delivery applications.

AUTHOR INFORMATION

Corresponding Author

*E-mail: maryam.tabrizian@mcgill.ca

Notes

The authors declare no competing financial interest.

ACKNOWLEDGMENTS

The authors would like to thank L. Mongeon for assistance with SEM imaging, V. Sivakumar for assistance with DNA release studies, and Dr. H. Durham for access to bacterial work facilities. This work was funded by a National Science and Engineering Research Council of Canada Discovery Grant and the Canadian Institutes of Health Research Regenerative Medicine Grant. C.A.H. is supported by a National Science and Engineering Research Council of Canada Graduate Scholarship.

REFERENCES

- (1) Segura, T.; Shea, L. D. *Bioconjugate Chem.* **2002**, *13*, 621–629.
- (2) Ziauddin, J.; Sabatini, D. M. *Nature* **2001**, *411*, 107–110.
- (3) Bengali, Z.; Pannier, A. K.; Segura, T.; Anderson, B. C.; Jang, J. H.; Mustoe, T. A.; Shea, L. D. *Biotechnol. Bioeng.* **2005**, *90*, 290–302.
- (4) Stachelek, S. J.; Song, C.; Alferiev, I.; Defelice, S.; Cui, X.; Connolly, J. M.; Bianco, R. W.; Levy, R. J. *Gene Ther.* **2004**, *11*, 15–24.
- (5) Decher, G. *Science* **1997**, *277*, 1232–1237.
- (6) Tang, Z.; Wang, Y.; Podsiadlo, P.; Kotov, N. A. *Adv. Mater.* **2006**, *18*, 3203–3224.
- (7) Jewell, C. M.; Lynn, D. M. *Adv. Drug Deliv. Rev.* **2008**, *60*, 979–999.
- (8) Blacklock, J.; You, Y. Z.; Zhou, Q. H.; Mao, G.; Oupicky, D. *Biomaterials* **2009**, *30*, 939–950.
- (9) Saurer, E. M.; Yamanouchi, D.; Liu, B.; Lynn, D. M. *Biomaterials* **2011**, *32*, 610–608.
- (10) Benkirane-Jessel, N.; Lavallo, P.; Hubsch, E.; Holl, V.; Senger, B.; Haikel, Y.; Voegel, J. C.; Ogier, J.; Schaaf, P. *Adv. Func. Mater.* **2005**, *15*, 648–654.

- (11) Jessel, N.; Oulad-Abdelghani, M.; Meyer, F.; Lavallo, P.; Haikel, Y.; Schaaf, P.; Voegel, J. C. *Proc. Natl. Acad. Sci. U.S.A.* **2006**, *103*, 8618–8621.
- (12) Zhang, J.; Chua, L. S.; Lynn, D. M. *Langmuir* **2004**, *20*, 8015–8021.
- (13) Jewell, C. M.; Zhang, J.; Fredin, N. J.; Lynn, D. M. *J. Controlled Release* **2005**, *106*, 214–223.
- (14) Cai, K.; Hu, Y.; Wang, Y.; Yang, L. *J. Biomed. Mater. Res. A* **2008**, *84*, 516–522.
- (15) Cai, K.; Hu, Y.; Luo, Z.; Kong, T.; Lai, M.; Sui, X.; Wang, Y.; Yang, L.; Deng, L. *Angew. Chem., Int. Ed. Engl.* **2008**, *47*, 7479–7481.
- (16) Lu, Z. Z.; Wu, J.; Sun, T. M.; Ji, J.; Yan, L. F.; Wang, J. *Biomaterials* **2008**, *29*, 733–741.
- (17) Yamauchi, F.; Kato, K.; Iwata, H. *Langmuir* **2005**, *21*, 8360–8367.
- (18) Meyer, F.; Ball, V.; Schaaf, P.; Voegel, J. C.; Ogier, J. *Biochim. Biophys. Acta* **2006**, *1758*, 419–422.
- (19) Dimitrova, M.; Arntz, Y.; Lavallo, P.; Meyer, F.; Wolf, M.; Schuster, C.; Haikel, Y.; Voegel, J. C.; Ogier, J. *Adv. Func. Mater.* **2007**, *7*, 233–245.
- (20) Bengali, Z.; Rea, J. C.; Gibly, R. F.; Shea, L. D. *Biotechnol. Bioeng.* **2009**, *102*, 1679–1691.
- (21) Rea, J. C.; Gibly, R. F.; Barron, A. E.; Shea, L. D. *Acta Biomater.* **2009**, *5*, 903–912.
- (22) Brito, L. A.; Chandrasekhar, S.; Little, S. R.; Amiji, M. M. *J. Biomed. Mater. Res. A* **2010**, *93*, 325–336.
- (23) Zhang, Q.; Cheng, S. X.; Zhang, X. Z.; Zhuo, R. X. *Macromol. Biosci.* **2009**, *9*, 1262–1271.
- (24) Yamauchi, F.; Koyamatsu, Y.; Kato, K.; Iwata, H. *Biomaterials* **2006**, *27*, 3497–3504.
- (25) Schneider, A.; Richert, L.; Francius, G.; Voegel, J. C.; Picart, C. *Biomed. Mater.* **2007**, *2*, S45–51.
- (26) Holmes, C. A.; Tabrizian, M. *J. Biomed. Mater. Res. A* **2012**, *100*, 518–526.
- (27) Son, K. K.; Tkach, D.; Patel, D. H. *Biochim. Biophys. Acta* **2000**, *1468*, 11–14.
- (28) Srinivasan, C.; Burgess, D. J. *J. Controlled Release* **2009**, *136*, 62–70.
- (29) Hsu, C. Y.; Uludağ, H. *BMC Biotechnol.* **2008**, *8*, 23.
- (30) Candiani, G.; Frigerio, M.; Viani, F.; Verpelli, C.; Sala, C.; Chiamenti, L.; Zaffaroni, N.; Folini, M.; Sani, M.; Panzeri, W.; Zanda, M. *ChemMedChem* **2007**, *2*, 292–296.
- (31) Ye, L.; Haider, H. K.; Tan, R.; Su, L.; Law, P. K.; Zhang, W.; Sim, E. K. *Biomaterials* **2008**, *29*, 2125–2137.
- (32) Decastro, M.; Saijoh, Y.; Schoenwolf, G. C. *Dev. Dyn.* **2006**, *235*, 2210–2219.
- (33) Michel, M.; Vautier, D.; Voegel, J. C.; Schaaf, P.; Ball, V. *Langmuir* **2004**, *20*, 4835–4839.
- (34) Leguen, E.; Chassepot, A.; Decher, G.; Schaaf, P.; Voegel, J. C.; Jessel, N. *Biomol. Eng.* **2007**, *24*, 33–41.